El Chichón about 600 years ago could have caused, or contributed to, the global cool period around A.D. 1300 (*10*). Compilation of data (*11*) correlating Greenland ice-core acidity peaks (*12*) with historic eruptions and unusual atmospheric phenomena in Europe includes two inadequately explained acidity peaks at A.D. 1258 (±1 year) and A.D. 623 (±3 years). We speculate that these peaks may reflect prehistoric explosive activity of El Chichón. Similarly, poorly explained "frost events" dated at A.D. 628, 687, 1171, and 1200 by La-Marche and Hirschboeck (*13*), who argue that frost damage in tree rings can record "climatically effective" eruptions, may be crudely correlated with the last two major eruptive episodes of El Chichón.

ROBERT I. TILLING
MEYER RUBIN
U.S. Geological Survey, National Center, Reston, Virginia 22092
HARALDUR SIGURDSSON
STEVEN CAREY
Graduate School of Oceanography, University of Rhode Island, Kingston 02881
WENDELL A. DUFFIELD
U.S. Geological Survey, Flagstaff, Arizona 86001
WILLIAM I. ROSE
Department of Geology and Geological Engineering, Michigan Technological University, Houghton 49931

References and Notes

1. M. Alcayde, Ed., *El Volcan Chichonal* (Instituto de Geología, Universidad Nacional Autónoma de México, Mexico City, 1983); H. Sigurdsson, S. N. Carey, J. M. Espindola, *J. Volcanol. Geotherm. Res.*, in press; J. M. Hoffer, F. Gomez, P. P. Muela, *Science* **218**, 1307 (1982); J. Varekamp and J. Luhr, *Eos* **63**, 1126 (1982).
2. W. A. Duffield, R. I. Tilling, R. Canul, *J. Volcanol. Geotherm. Res.* **20**, 117 (1984).
3. J. M. Mitchell, *Weatherwise* **35**, 252 (1982); C. R. Nagaraja and W. A. Bradley, *Geophys. Res. Lett.* **10**, 389 (1983); O. B. Toon, *Eos* **63**, 901 (1982); D. E. Parker and J. L. Brownscombe, *Nature (London)* **301**, 406 (1983); E. J. Mroz and W. A. Sedlacek, *Eos* **63**, 900 (1982); S. Self, M. R. Rampino, J. J. Barbera, *J. Volcanol. Geotherm. Res.* **11**, 41 (1981); W. A. Sedlacek, E. J. Mroz, A. L. Lazrus, B. W. Gandrud, *J. Geophys. Res.* **88**, 3741 (1983).
4. F. Mullerreid, *Z. Vulkanol.* **14**, 191 (1932).
5. P. E. Damon and E. Montesinos, *Ariz. Geol. Soc. Dig.* **11**, 155 (1978).
6. R. Canul and V. S. Rocha, unpublished report of the Geothermal Department of the Comisión Federal de Electricidad, Morelia, Michoacan, Mexico, September 1981.
7. J. J. Cochemé, A. Demant, W. A. Duffield, J. Guerrero, L. Silva, R. I. Tilling, *C. R. Acad. Sci. Paris Ser. II* **295**, 737 (1982); J. Luhr, I. S. E. Carmichael, J. Varekamp, *J. Volcanol. Geotherm. Res.*, in press; W. I. Rose *et al.*, *ibid.*, in press; J. J. McGee and R. I. Tilling, *Eos* **64**, 893 (1983).
8. M. Stuiver, *Radiocarbon* **24**, 1 (1982).
9. R. S. Santley and J. Sabloff, personal communication.
10. L. M. Libby, *Past Climates: Tree Thermometers, Commodities, and People* (Univ. of Texas Press, Austin, 1983), pp. 28–68; P. Bergthorsson, Ed., *Proceedings of the Conference on Climate in the 11th to 16th Centuries* (National Center for Atmospheric Research, Boulder, Colo., 1962).
11. R. B. Stothers and M. R. Rampino, *Science* **222**, 411 (1983).
12. C. V. Hammer, H. B. Clausen, W. Dansgaard, *Nature (London)* **288**, 230 (1980).
13. V. C. LaMarche, Jr., and K. K. Hirschboeck, *ibid.* **307**, 121 (1984).
14. We greatly appreciate the scientific and logistical support of the following individuals and institutions: J.-J. Cochemé, L. Silva, and J. Guerrero, Instituto de Geología, UNAM; S. de la Cruz-Reyna, Instituto de Geofísica, UNAM; R. Riva Palacio, Comisión Federal de Electricidad, Tuxtla Gutierrez; and the governments of Tabasco and Chiapas states. This cooperative study was supported in part by NSF grants EAR-8205606 and INT-8305779, NASA grant NAG 1-200, and the Office of Foreign Disaster Assistance of USAID.

23 December 1983; accepted 6 March 1984

Single-Crystal Elastic Properties of the Modified Spinel (Beta) Phase of Magnesium Orthosilicate

Abstract. *The single-crystal elastic moduli of the modified spinel structure (beta phase) of magnesium orthosilicate (Mg_2SiO_4) have been measured by Brillouin spectroscopy under ambient conditions. Single crystals with dimensions up to 500 micrometers were grown at 22 gigapascals and 2000°C over a period of 1 hour. Growth of crystals larger than 100 micrometers was achieved only when the pressure was within 5 percent of the pressure of the phase boundary separating the beta- and gamma-phase stability fields. A comparison of the elastic properties of the modified spinel phase with those of the olivine phase suggests that the 400-kilometer seismic discontinuity in the earth's mantle can be described by a mantle with 40 percent olivine. These results confirm that the 400-kilometer discontinuity can be due to the transition from olivine to modified spinel. The amount of olivine that must be present is less than that in a pyrolite model, although the results do not exclude pyrolite as a possible mantle model.*

Earth scientists have recognized for over half a century that the earth's mantle must have some vertical layering, which results from either chemical heterogeneities or phase transformations (*1*). The exact nature and location of this heterogeneity have implications concerning the origin and history of the earth and the current mode of evolution.

Thirty years ago, Francis Birch (*2*) demonstrated that the change in seismic velocities in the transition zone (at a depth of 400 to 800 km) required that phase transformations were present in this region. Laboratory high-pressure, high-temperature capabilities have continued to expand as the seismic resolution has improved. The transition zone is now recognized as consisting of at least two sharp velocity increases, one at a depth of 400 km and the other at 670 km (*3*). Laboratory studies have demonstrated that olivine and pyroxene undergo a number of phase transformations at pressures associated with these depths in the earth (*4*). A notable transformation is the change from olivine to a modified spinel structure (beta phase) and at higher pressures to a spinel structure (gamma phase). The first of these transformations has become associated with the 400-km seismic discontinuity in the mantle since the pressure-temperature regime of the transformation is appropriate to that depth. Further assessments of this discontinuity in the earth require laboratory measurements of the acoustic velocities of the high-pressure phase for comparison with the in situ seismic observations.

We present here the results of a laboratory determination of the single-crystal elastic properties of the modified spinel structure of Mg_2SiO_4. These properties define the acoustic velocities in polycrystalline samples as well as in single crystals and are thus appropriate to compare with the seismically determined velocities within the earth's transition zone.

It is now possible to make these measurements because of recent developments in two experimental programs over the past 10 years. One program is the development of large-volume, high-pressure equipment capable of 24 GPa and 2400°C. At Nagoya University these conditions were generated with the use of a multianvil pressure apparatus driven by a pair of guide blocks in a uniaxial press that can provide a ram load of 15,000 tons. In order to grow single crystals larger than 100 μm, we must generate such high pressures and temperatures with fluctuations of no more than a few percent on sufficiently large volumes. The high temperatures are achieved by electrical furnaces consisting of concentric cylindrical sleeves of graphite and $LaCrO_3$. During the early stages of the heating cycle, the graphite supplies most of the heat. However, $LaCrO_3$ is a semiconductor, and above a few hundred degrees it will contribute to the heating. At about 1000°C, graphite transforms to diamond and the $LaCrO_3$

Table 1. Single-crystal elastic moduli of the modified spinel (beta phase) of Mg_2SiO_4; C_{ij}, elastic stiffness constants; S_{ij}, elastic compliance.

ij	C_{ij} (Mbar)	S_{ij} ($Mbar^{-1}$)
11	3.60 ± 0.06	0.320
22	3.83 ± 0.04	0.295
33	2.73 ± 0.05	0.453
44	1.12 ± 0.02	0.895
55	1.18 ± 0.04	0.847
66	0.98 ± 0.04	1.017
12	0.75 ± 0.09	−0.030
13	1.10 ± 0.06	−0.117
23	1.05 ± 0.09	−0.102

must supply all the heat above this temperature. The conditions must remain stable for an hour and be reproducible so that synthesis conditions can be explored in pressure and temperature. This development has made possible the synthesis of single crystals of high-pressure phases with dimensions up to 500 μm.

The other program is the utilization of Brillouin spectroscopy for the elastic characterization of microcrystals. This experimental development allows measurements to be performed on single crystals as small as 100 μm (*5*). Brillouin scattering is the scattering of light (photons) by acoustic waves (phonons). The frequency of the scattered light is Doppler-shifted as compared to the incident light because the scatterer is moving (or due to the conservation of energy). The measurement of the frequency shift thus yields the velocity of the scattering acoustic wave. Rotation of the crystal relative to the optical system gives a measure of acoustic velocity as a function of crystallographic direction. The system used in our experiments included an argon-ion laser, a Fabry-Perot interferometer operated in a triple-pass configuration, a three-circle x-ray goniometer for mounting the sample, and a photomultiplier with associated optical and electronic elements. Other aspects of the technique have been described (*5, 6*). The more traditional means of measuring acoustic velocities involve introducing a mechanical disturbance into a sample and measuring the time of flight of this disturbance. Brillouin scattering measurements can be accomplished on samples with volumes one-millionth the size required by such techniques.

The elasticity data for the beta phase were obtaied from two single crystals. One crystal measured approximately 300 by 200 by 150 μm^3, and the other measured 150 by 100 by 100 μm^3. No crystal faces were developed on these samples. The samples do contain a small amount of very fine inclusions or defects. These inclusions were manifest as a source of parasitic light scattering. However, the inclusions were not visible with a microscope. Thus the density of inclusions or defects is quite small, and we expect no effect on the measured acoustic properties. The samples were oriented with an automated four-circle x-ray diffractometer. The orientation is preserved upon transfer to the Brillouin spectrometer to about 0.5°. The x-ray density was determined (3.474 g/cm^3), the lattice constants being 5.696(1), 11.453(1), and 8.256(1). These results are in good argument with reported values (*7*). The refractive indices (n_a, n_b, and n_c) for the beta phase are 1.672, 1.696, and 1.683, respectively (*8*).

The samples were grown under conditions of about 21 GPa and 2000°C. Single crystals larger than 100 μm could be grown only when the pressure was within about 5 percent of the pressure of the phase boundary between the beta and gamma phase. Outside this region, the crystal size was less than 30 μm.

The beta phase is orthorhombic and requires nine elastic moduli to completely specify its elastic properties. A total of 38 acoustic longitudinal and shear-wave velocities were determined for 19 propagation directions from over 100 recorded Brillouin spectra. We invented these data, using the method described by Weidner and Carleton (*5*), to obtain the elastic moduli (Table 1). Data for individual velocities are compared with the model velocities in Fig. 1. The model and observed velocities differ by 0.08 km/sec in a root-mean-square sense. Each elastic modulus was determined to be independently defined by the measured acoustic velocity, as the largest linear trade-off coefficient (*5*) was less than 0.005.

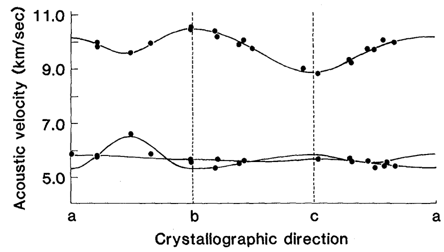

Fig. 1. Acoustic velocities of the modified spinel (beta phase), Mg_2SiO_4. The measured values are projected onto the nearest principal plane. The solid lines are the calculated values based on the deduced elastic moduli.

To our knowledge, these are the first reported acoustic velocity data for the beta phase of magnesium orthosilicate. Table 2 compares the range of elastic properties and acoustic velocities that would be observed in a polycrystalline aggregate of the beta phase with those for olivine (alpha phase) (*9*) of the same composition. These data correspond to atmospheric pressure and room temperature for the pure magnesium end-member. In the earth's mantle at a depth of 400 km none of these conditions will be appropriate. The pressures will exceed 100 kbar, the temperature will exceed 1000°C, and the olivine component should contain 10 to 20 percent iron. However, each of these variables will have a similar effect on the acoustic velocities of both phases. Thus, the difference in acoustic velocities between the two phases is the most stable quantity for comparison with the observed seismic velocities at this depth.

If the seismic discontinuity at 400 km is due to the transition from the olivine to the modified spinel structure, then the magnitude of the discontinuity should be related to a difference in acoustic velocities of these two phases along with the volume fraction of the olivine component present at this depth. Since other minerals will also experience phase transformations in this region, we can specify an upper bound on the amount of the olivine component at this depth.

The range of the magnitude of the discontinuity reported in the literature is quite large. However, the seismic data base of these different observations have different sensitivities to the size of the discontinuity. In this report, we choose specific body-wave studies that use

Table 2. Aggregate elastic properties of the beta and olivine phases of Mg_2SiO_4. The olivine data are from Kumazawa and Anderson (*9*). Abbreviations: VRH, Voigt-Reuss-Hill; V_p, longitudinal wave velocity; V_s, shear wave velocity; K, bulk modulus; and μ, shear modulus.

Source	V_p (km/sec)	V_s (km/sec)	K (Mbar)	μ (Mbar)
		Beta phase		
Reuss	9.63	5.67	1.73	1.12
Voigt	9.72	5.74	1.75	1.15
VRH	9.66	5.71	1.74	1.14
		Olivine phase		
Reuss	8.49	4.96	1.27	0.79
Voigt	8.64	5.06	1.31	0.83
VRH	8.57	5.01	1.29	0.81

wave-form analysis to compare with our laboratory data. Although these data may not be representative of all the reported seismic observations, they are probably the most sensitive to the features that we utilize and serve to illustrate the utility of our data in interpreting the seismic structure of the mantle.

Let us compare the differences in acoustic velocities between the olivine and modified spinel phase as deduced in this report with reported velocity discontinuities at 400 km in the mantle. The seismic compressional discontinuity of 0.43 km/sec (*10*) is about 40 percent of the difference between the two phases (1.06 km/sec). The seismic shear discontinuity of 0.23 km/sec (*11*) is about 35 percent of this difference (0.71 km/sec). This comparison suggests an olivine content of the mantle of 40 percent by volume, with the other 60 percent being composed of minerals that do not undergo phase transformations at this depth. This amount of olivine is low compared to that of most pyrolite mantle models, which generally require that olivine represent over 60 percent of the total volume (*4*). The pressure dependence of the velocity difference between the olivine and the beta phase is probably the greatest experimental uncertainty, and the magnitude of the velocity discontinuity is the greatest observational uncertainty. If the pressure derivatives of the bulk and shear moduli for the beta phase are approximately 3.9 and 1.1, then the observed discontinuity is consistent with a pyrolite composition. This compares to values of 5.3 and 1.8 for olivine. Although these inferred values are lower than expected, they are not sufficiently unreasonable to warrant rejecting the pyrolite model. We conclude that, although pyrolite is still an acceptable mantle model, a model with less olivine is preferable.

HIROSHI SAWAMOTO*
DONALD J. WEIDNER
SATOSHI SASAKI†
MINEO KUMAZAWA‡
Department of Earth and Space Sciences, State University of New York, Stony Brook 11794

References and Notes

1. K. Bullen, *An Introduction to the Theory of Seismology* (Cambridge Univ. Press, Cambridge, ed. 3, 1963).
2. F. Birch, *J. Geophys. Res.* **57**, 227 (1952).
3. L. R. Johnson, *ibid.* **72**, 6309 (1967).
4. A. E. Ringwood, *Composition and Petrology of the Earth's Mantle* (McGraw-Hill, New York, 1975).
5. D. J. Weidner and H. R. Carleton, *J. Geophys. Res.* **82**, 1334 (1977).
6. D. J. Weidner, H. Wang, J. Ito, *Phys. Earth Planet. Inter.* **17**, 7 (1978); D. J. Weidner and M. T. Vaughan, in *High-Pressure Science and Technology*, D. Timmerhaus and M. S. Barber, Eds. (Plenum, New York, 1979), vol. 2, p. 85.
7. H. Horiuchi and H. Sawamoto, *Am. Mineral.* **66**, 568 (1981).
8. H. Sawamoto, H. Horiuchi, M. Tokonami, M. Kumazawa, paper presented at the U.S.–Japan Seminar on High-Pressure Research: Applications in Geophysics, Hakone, Japan, 1981 (program with abstracts, p. 68).
9. M. Kumazawa and O. L. Anderson, *J. Geophys. Res.* **74**, 5961 (1969).
10. L. J. Burdick, *ibid.* **86**, 5926 (1981).
11. S. P. Grand and D. V. Helmberger, *Geophys. J. R. Astron. Soc.* **76**, 399 (1984).
12. This research was supported by NSF grant EAR-8120954 and Japan Society for the Promotion of Science Study Abroad program.
* Present address: Department of Earth Sciences, Nagoya University, Nagoya 464, Japan.
† Present address: Photon Factory, National Laboratory for High-Energy Physics, Oho-Machi, Ibaraki 305, Japan.
‡ Present address: Geophysical Institute, Faculty of Science, University of Tokyo, Tokyo, Japan.

21 November 1983; accepted 14 March 1984

A Candidate Magnetic Sense Organ in the Yellowfin Tuna, *Thunnus albacares*

Abstract. *Single-domain magnetite crystals have been isolated and characterized from tissue located in a sinus within the dermethmoid bone of the skull of the yellowfin tuna,* Thunnus albacares. *Their chemical composition, narrow size distribution, and distinctive crystal morphology indicate that these crystals are biochemical precipitates. Experiments on the interaction between particles reveal the organization of the particles in situ and suggest a possible form for candidate magnetoreceptor organelles. The consistent localization of such particles with similar arrangement within the dermethmoids of this and other pelagic fishes suggests that the ethmoid region is a possible location for a vertebrate magnetic sense organ.*

Magnetic material has been detected in the tissues of various metazoan species (*1–5*). Although the material is inferred to be magnetite, in many cases this has not yet been established, and external contaminants have not been excluded as possible sources of magnetic remanence. Even in the homing pigeon and the honey bee, detailed localization of the magnetite has proved difficult to ascertain, and the particles have not been isolated or characterized previously (*3, 4*). For many of the species studied, behavioral evidence for magnetic sensitivity is lacking or in dispute.

Earlier we reported reproducible conditioned responses to earth-strength magnetic fields in the yellowfin tuna, *Thunnus albacares* (*6*). We now report the detection, extraction, and characterization of magnetite crystals from tissue within a sinus formed by the dermethmoid bone of the skull of this species. The crystals have a narrow size distribution, are single magnetic domains, and have morphologies similar to other biochemically formed magnetites. Studies of the interactions between particles suggest that the crystals are arranged in groups or chains in the dermethmoid tissue. Magnetite-based magnetoreceptor organelles arranged in vivo in a form consistent with these observations could provide these fish with a sensitive magnetoreception system.

To distinguish magnetic material with a possible magnetoreceptive function from other deposits, we sought to identify a tissue with the following characteristics: (i) it should have a high remanent magnetic moment concentrated in a small volume of sample compared with other tissues from the same fish; (ii) the anatomical position of the magnetic tissue must be consistent from fish to fish; (iii) the bulk magnetic properties, including particle coercivity, should be similar in different individuals and in different species of fish; and (iv) it should be innervated.

Tissue and organ samples, including bones of the body and the skull, skin, sense organs, viscera, and swimming muscles, were dissected from three 1-year-old yellowfin tuna (fork length, 40 to 50 cm) with glass microtome knives and handled with nonmetallic tools in a magnetically shielded, dust-free clean room. Although subsequent dissections focused on the most magnetic tissue, other samples were measured in all fish. Samples were washed in glass-distilled water, frozen in liquid nitrogen, exposed to strong fields from a cobalt-samarium magnet or an air-core impulse solenoid (*7*), and tested for isothermal remanent magnetization (IRM) in a superconducting magnetometer. We extracted the magnetic material for other tests by combining the magnetic tissue from several fish, grinding the tissues in a glass tissue grinder, extracting released fats with ether, digesting the remaining cellular material in Millipore filtered 5 percent sodium hypochlorite solution (commercial bleach), and briefly treating the residue with 0.5*M* EDTA (*p*H 7.1). After centrifuging and washing, aggregates of black particles could be separated magnetically from the residue; control samples of originally nonmagnetic tissues yielded no such product. The magnetic